THE JOURNAL OF PHYSICAL CHEMISTRY C

Article

pubs.acs.org/JPCC

Thermal Conductivity of M@C_{82} [M = Dy, Gd] Thin Films

Trisha Mondal,[†] Ajay Tripathi,[†] Jinying Zhang,[‡] Thoudinja Shripathi,[§] Hisanori Shinohara,[∥] and Archana Tiwari*[,†]

[†]Department of Physics, School of Physical Sciences, Sikkim University, Gangtok, Sikkim 737102, India

[‡]Center of Nanomaterials for Renewable Energy, State Key Laboratory of Electrical Insulation and Power Equipment, School of Electrical Engineering, Xian Jiaotong University, Xian 710054, Shaanxi, China

[§]UGC-DAE CSR, Indore Centre, Khandwa Road, Indore 452001, M.P., India

[∥]Department of Chemistry and Institute for Advanced Research, Nagoya University, Nagoya 464-8602, Japan

Supporting Information

ABSTRACT: Temperature dependent Raman spectra of a Dy@C_{82} thin film are investigated between 80 and 300 K. The first order temperature coefficient is evaluated for both Dy−C and C−C vibrational modes which reveals the presence of thermal and anharmonic contributions to the phonon hardening at low temperatures. The Dy−C mode broadens while decreasing the temperature revealing that the electron−phonon coupling is dominant over phonon−phonon coupling at low temperatures. In addition, laser-power dependent Raman spectra of Dy@C_{82} and Gd@C_{82} have been analyzed for estimating their first order power coefficients and the thermal conductivities.

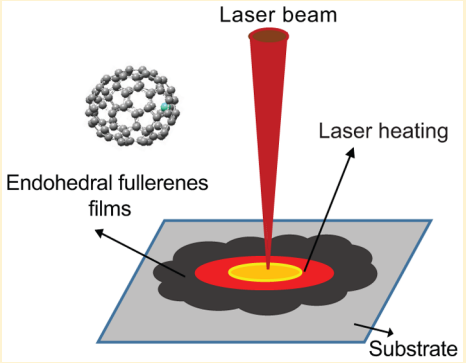

INTRODUCTION

Thermoelectrics have a wide range of applications in power generation and thermal insulation in solid state memory devices.[1−3] Their efficiency is often defined by the figure of merit which is inversely proportional to the thermal conductivity and electrical resistivity.[4,5] Many works have been done in order to identify suitable nano, bulk, and hybrid materials with enhanced thermoelectric properties.[6−8] For a bulk material, these properties can be refined by either reducing its thermal conductivity by inducing phonon scattering or by increasing its figure of merit via doping lower-dimensional structures such as fullerenes in its matrix.[8−10]

Both C_{60} and C_{70} fullerenes and their derivatives offer low to ultra low thermal conductivities at room temperature which are nearly independent of the sample thickness and the substrates.[11,12] This is why, they are potential candidates for thermoelectric and thermal insulation applications. Even though thermal conductivity of C_{60} and its derivatives has been extensively examined, the reports on that of the larger fullerenes such as endohedral metallofullerenes, M@C_{82} is limited. These fullerenes, with a metal (M) ion encapsulated inside a hollow fullerene cage, possess interesting electronic, optical, and magnetic properties and offer several applications in the field of electronics, spintronics, optoelectronics, and biomedicines.[13−16]

In order to realize scalable fullerene-based thermoelectric systems, the cages with opposite signs of the thermopower should be arranged in series.[17,18] Although the linear arrangement of the cages can be attained inside the carbon nanotubes, the thermopower cannot be regulated without changing their chemical compositions.[17,19,20] Recent reports have shown that endohedral metallofullerene $Sc_3N@C_{80}$ has potential applications in thermoelectrics as it exhibits sign-tunable thermopower which can be modulated by the mechanical pressure.[17,18,21] In addition to the cage mediated thermal transport, the metallofullerenes may present an additional transport mechanism via metal−cage interaction and thereby may regulate the thermal conductivities and thermoelectric properties of the bare fullerenes.[22]

Raman spectroscopy has been proven effective in measuring the metal-cage interaction strength, their bond length, force constant and oxidation state of the metal ion inside fullerenes.[23−27] Being a noncontact and nondestructive technique, it has also been employed on several thin-films and nanomaterials for the reliable estimation of their thermal conductivities.[28−32]

Here, we communicate temperature dependent Raman studies of a Dy@C_{82} thin film. The first order temperature coefficients are evaluated for Dy−C and C−C vibrations. In addition, we also present the first report on the thermal conductivity measurements of the thin films of Dy@C_{82} and Gd@C_{82} fullerenes using both temperature and laser-power dependent Raman spectroscopy. This study provides insight into the interplay between thermal and mechanical transformations experienced by the material while

Received: December 14, 2016
Revised: January 21, 2017
Published: January 23, 2017

DOI: 10.1021/acs.jpcc.6b12577
J. Phys. Chem. C 2017, 121, 3642−3647

changing the temperature and thereby assessing their suitability toward thermoelectric applications.

MATERIALS AND METHODS

Isomer specific Dy@C_{82}(>96.5%) and Gd@C_{82}(>98.5%) were dissolved in CS_2 and were drop-casted into thin-films (having thickness ∼0.37 mm) on the glass substrate for the Raman measurements. (See Figure S1 for the purity of the fullerenes and their isotopic distribution.)

Temperature-dependent Raman spectra were recorded using a LABRAM HR-800 spectrometer with an excitation wavelength of 633 nm. The thin-flims were mounted in THMS-600 stage (Linkam, U.K.) where the temperature was varied between 80 and 300 K in a thermal step of 10 K and having a temperature stability of ±0.1 K. Throughout the measurement, 2 mW laser power was imposed on the film.

Laser power-dependent Raman measurements were performed at room temperature using Renishaw inVia RM2000 spectrometer at an excitation wavelength of 785 nm (having laser spot size ∼1.5 μm) and the laser power was varied between 0.15 and 15 mW.

RESULTS AND DISCUSSION

Temperature−Dependent Raman Spectral Analysis of Dy@C_{82}. In general, two kinds of vibrations are reported in the metallofullerenes: (a) Raman shifts below 200 cm^{-1} attributed to metal−cage vibrations and (b) Raman shifts above 200 cm^{-1} assigned to the cage internal vibrations.[24,25] Raman spectra of Dy@C_{82} in the temperature range 80−300 K are shown in Figure 1. At 300 K, three distinct Raman peaks are observed at

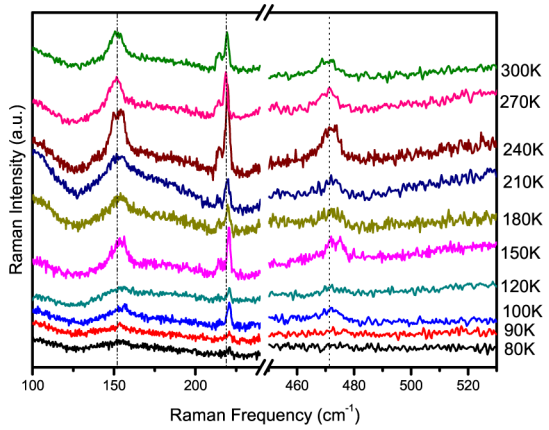

Figure 1. Temperature dependent Raman spectra of Dy@C_{82} obtained between 80 and 300 K with excitation wavelength of 633 nm.

151.5(1), 219.4(1), and 470.9(3) cm^{-1} revealing the presence of both kinds of vibrations in Dy@C_{82}. In addition to these peaks, a weak peak at 215 cm^{-1} is also observed. However, due to its weak intensity, the 215 cm^{-1} peak has not been analyzed in the temperature dependent Raman studies.

Upon decreasing the temperature to 100 K, the Raman peaks are blue-shifted and are observed at 153.8(5), 220.6(1), and 473.0(4) cm^{-1}, respectively. At 80 K, only two peaks at 154.5(8) and 220.6(3) cm^{-1} are observed revealing a continued blue-shift in their energies while lowering the temperature. At 80 K, 471 cm^{-1} peak becomes indistinguishable due to line broadening. The thermal variation of the peak positions at ∼151, 219, and 471 cm^{-1} are illustrated in Figure 2. The shift in Raman frequencies (ω) with temperature has been fitted with the following equation:[28,29]

$$\omega(T) = \omega_0 + \chi_T T \quad (1)$$

where ω_0 is the frequency at absolute zero and χ_T is the first order temperature coefficient. The higher order coefficients have been neglected as the thermal analysis is performed at low temperatures. The thermal variation of Raman peaks at 151, 219, and 471 cm^{-1} are fitted with the above equation (see Figure 2) and the fitting parameters ω_0 and χ_T are evaluated. The ω_0 for 151, 219, and 471 cm^{-1} peaks are found to be 155.4(6) cm^{-1}, 221.4(2) cm^{-1} and 473.7(4) cm^{-1} respectively whereas χ_T for the respective peaks are found to be −0.013(1), −0.007(2), and −0.008(1) cm^{-1}/K. The negative temperature coefficients of metal-cage and cage internal vibrations in these fullerenes may be attributed to the thermal expansion of the cage and anharmonicity in the lattice forces.[33,34] Both properties influence the bond length and the interatomic interaction strength upon varying the temperature. Similar observations on Gd@C_{82} have been reported previously where the metal-cage distance changes with temperature.[35] Like Gd@C_{82},[27] the total angular momentum J of Dy@C_{82} is found to be constant (∼3.7) above 40 K revealing that the oxidation state of Dy^{3+} remains invariant (see Figure S2) and does not contribute toward the observed phonon hardening at the examined temperatures.

The χ_T for Gd−C vibration is higher than that of the Dy−C in C_{82} cage.[27] This could be credited to the larger ionic size of Gd^{3+} than that of Dy^{3+} due to which Gd−C suffers stronger compression than Dy−C in the rigid cage.[36−38] χ_T for C_{82} cage internal vibrations (C−C) are similar irrespective of the encapsulated metal ion. Both fullerenes and carbon nanotubes have high bending strain energy which refrains the softening of C−C bonds with temperature and stem for smaller χ_T than those observed for graphene and other planar nanostructures.[28,33,34,39,40]

In addition to the thermal variations in the Raman frequencies, the temperature dependent line broadening was also examined for the metal-cage vibration (151 cm^{-1}) and the cage internal vibrations (219 and 471 cm^{-1}). Figure 3 shows the temperature dependent full width at half maxima (fwhm) of 151, 219, and 471 cm^{-1} peaks. At room temperature, the line width was found to be 2.3(2) and 6.2(4) cm^{-1} for 219 and 471 cm^{-1} peaks, respectively. From Figure 3a, it is evident that their line widths are nearly temperature independent whereas that of 151 cm^{-1} peak increases with decrease in temperature. The line width of a phonon in a crystalline lattice is determined by its interaction with other elementary excitations. In most of the materials temperature dependent line broadening occurs due to anharmonic effects and phonon−phonon interaction which can be written as[41,42]

$$\Gamma^{\mathrm{ph-ph}}(T) = \Gamma_0^{\mathrm{ph-ph}}\left[1 + \frac{2}{\exp\left(\frac{\hbar\omega_0}{2k_B T}\right) - 1}\right]$$

where $\Gamma^{\mathrm{ph-ph}}(T)$ is the temperature dependent line width arising due to anharmonic phonon−phonon (ph-ph) coupling and $\Gamma_0^{\mathrm{ph-ph}}$ is the temperature independent line width. We attempted to fit the temperature dependent fwhm of 151 cm^{-1} peak considering anharmonic phonon−phonon coupling only which is shown in Figure 3b. At low temperatures $\Gamma^{\mathrm{ph-ph}}(T)$ does not fit well with the experimental data revealing that other elementary excitations such as electrons, holes, or electron−hole pairs might

DOI: 10.1021/acs.jpcc.6b12577
J. Phys. Chem. C 2017, 121, 3642−3647

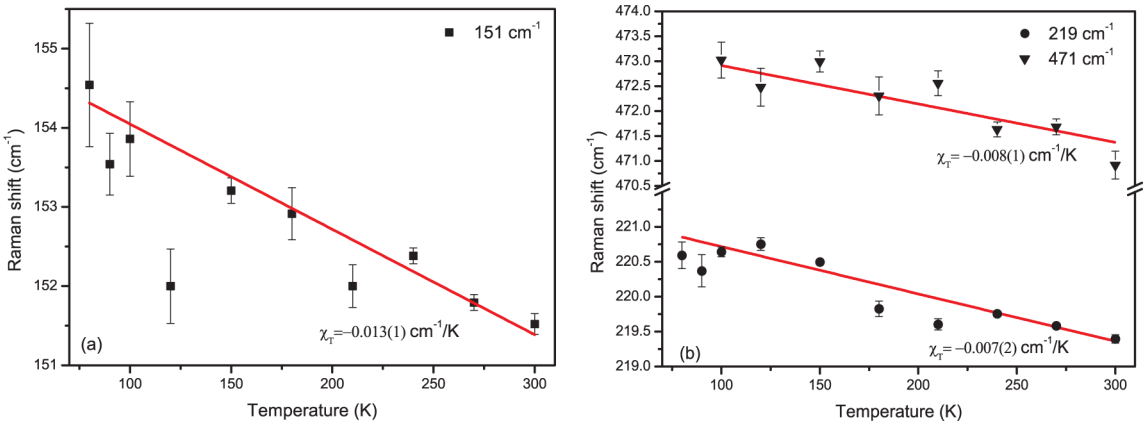

Figure 2. Temperature dependent Raman peak shifts observed at (a) 151 cm^{-1} and (b) 219 and 471 cm^{-1} due to Dy−C and C−C vibrational modes, respectively.

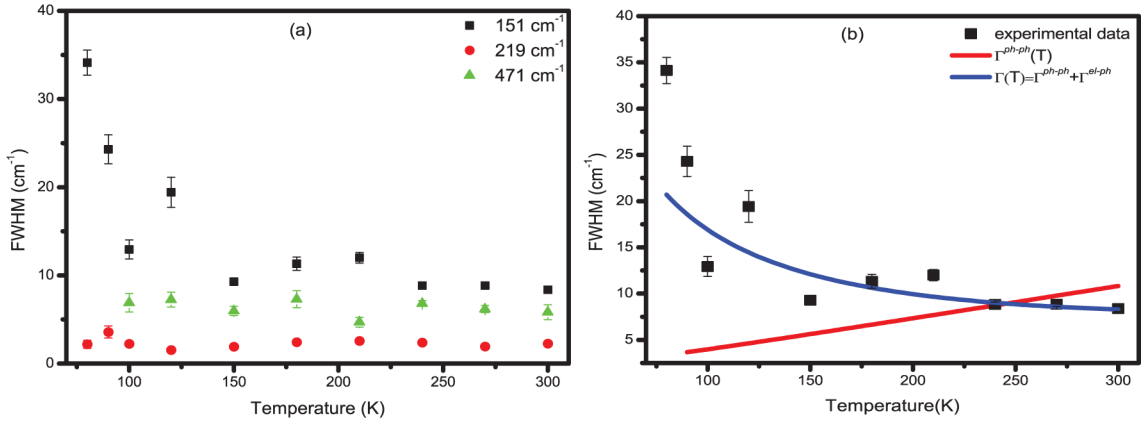

Figure 3. (a) Temperature dependent fwhm of 151, 219, and 471 cm^{-1} peak of $Dy@C_{82}$. (b) The temperature variation of fwhm of Dy−C vibrational mode (151 cm^{-1}) along with the fit of the data which includes both phonon−phonon and electron−phonon coupling in the line broadening.

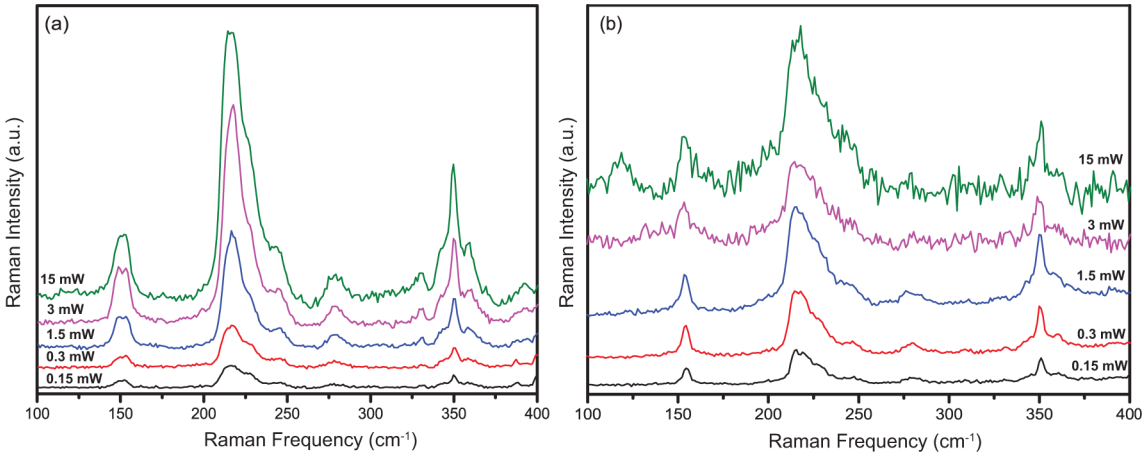

Figure 4. Laser power dependent Raman spectra of (a) $Dy@C_{82}$ and (b) $Gd@C_{82}$.

be interacting with the phonons. This is why we have redefined the thermal variation of fwhm by $\Gamma(T) = \Gamma^{ph-ph}(T) + \Gamma^{el-ph}(T)$, where $\Gamma^{el-ph}(T)$ is the line width due to electron−phonon (el-ph) coupling. $\Gamma^{el-ph}(T)$ is given by[43−46]

$$\Gamma^{el-ph} = \Gamma_0^{el-ph}\left[\frac{1}{\exp\left(-\frac{\hbar\omega_0}{2k_BT}\right)+1} - \frac{1}{\exp\left(\frac{\hbar\omega_0}{2k_BT}\right)+1}\right]$$

where Γ_0^{el-ph} is the line width due to electron−phonon coupling at 0 K. $\Gamma(T)$ is used to fit the experimental data and is shown in Figure 3(b). The fitting parameters Γ_0^{ph-ph} and Γ_0^{el-ph} are found to be 0.5(3) and 31(6) cm^{-1} respectively. Having $\Gamma_0^{el-ph} \gg \Gamma_0^{ph-ph}$ reveals that at low temperatures electron−phonon coupling dominates over phonon−phonon coupling and thus broadens the peak attributed to Dy−C vibration. At low temperatures, the thermal excitation of the electrons are overpowered by the generation of electron−hole pairs via phonon excitation. This in

DOI: 10.1021/acs.jpcc.6b12577
J. Phys. Chem. C 2017, 121, 3642−3647

turn, decreases the phonon lifetime and results in the line broadening.[43,47]

Thermal Conductivity of Dy@C_{82} and Gd@C_{82}. Raman spectroscopy is often used as noncontact mode for determining the thermal conductivity of thin films.[34,40,48] The combinational effect of temperature and laser power on phonon frequencies are used for the reliable evaluation of the thermal conductivity.[39,40,49]

The laser-power-dependent Raman spectra of Dy@C_{82} and Gd@C_{82} have been obtained at room temperature and are shown in Figure 4. The metal-cage vibration is observed at 151 cm^{-1} for Dy@C_{82} and at 154.4 cm^{-1} for Gd@C_{82} while using 785 nm excitation and having a laser power of 0.15 mW whereas C−C vibration for Dy@C_{82} and Gd@C_{82} are observed at 216.7 and 217.2 cm^{-1} respectively. These peaks are examined while changing the laser power and their variation is plotted in Figure 5. Upon increasing the laser power to 3 mW, the peak at 151 cm^{-1} linearly shifts by −0.4(2) cm^{-1} for Dy@C_{82} whereas the peak at 154.4 cm^{-1} shifts by −0.8(1) cm^{-1} for Gd@C_{82}. Above 3 mW, nonlinear peak shift is observed in the metal−cage vibration modes. The line widths of Dy−C and Gd−C vibrations at 0.15 mW are found to be 9.7(5) cm^{-1} and 5.0(2) cm^{-1} whereas at 3 mW, the line widths marginally expand to 11(1) and 7(1) cm^{-1} respectively. Upon increasing the power to 15 mW, the peak at 216.7 cm^{-1} shifts by −1.6(2)cm^{-1} for Dy@C_{82} and peak at 217.2 cm^{-1} shifts by −1.1(1) cm^{-1} for Gd@C_{82}. It is apparent that increase in the laser power locally heats the fullerenes and roots for redshift in the observed frequencies. Both the metal−cage and cage internal vibrations shift linearly with the laser power and exhibit a negative slope. The power dependent shift in the peak position, $\Delta\omega(P)$ is characterized by[40]

$$\Delta\omega(P) = \chi_P \Delta P \tag{2}$$

where χ_P is the first order power coefficient and ΔP is the change in the laser power. The observed variation in the Raman peak frequencies with the laser power is fitted with the above equation and the respective χ_P is evaluated. χ_P is found to be −0.3(1) cm^{-1}/mW for Dy−C vibration in Dy@C_{82} and −0.25(7) cm^{-1}/mW for Gd−C vibration in Gd@C_{82}. The power coefficients of these metallofullerenes are smaller than those reported for carbon nanotubes and the layered nanostructures such as graphene and MoS_2.[34,40,50] χ_P of C−C vibration in Dy@C_{82} and Gd@C_{82} are found to be −0.10(2) and −0.10(4) cm^{-1}/mW, respectively. For cage internal modes of vibrations, similar χ_P is obtained for both metallofullerenes which could be attributed to the presence of the same skeletal cage C_{82}.

While performing the Raman measurements, the laser beam causes local heating effect on the surface of the film which increases the surface temperature and eventually leads to thermal conductivity. When the film thickness is at least one order larger than the diameter of the laser source, the heat could be transferred radially through the film.[32,51] For such heat flow with hemishepherical distribution of isotherms on the film, the conventional heat flow equation of thermal conductivity (κ) can be written as[32,51,52]

$$\kappa = \frac{2P}{\pi a(T_l - T_b)} \tag{3}$$

where a is the laser beam diameter, T_b is the bulk sample temperature, and T_l is the local temperature on the surface due to the heating effects by the laser power P. In C_{60}, κ is weakly affected by the high frequency intramolecular phonons as compared to that of the low frequency ones.[53] This is why, in order to determine κ of Dy@C_{82} and Gd@C_{82}, we have considered the changes in the metal−cage vibration frequencies upon laser heating. For evaluating T_l and thus, κ of Dy@C_{82} and Gd@C_{82}, χ_T of Dy−C and Gd−C vibrations are extracted from this and the previous work respectively which are performed at low temperatures (80−300 K).[27] As the thermal variation in the Raman frequencies is linear, its slope χ_T and the laser-power dependent shifts in the Raman frequencies can be utilized for evaluating T_l of the samples. For instance, at 15 mW, T_l of Dy@C_{82} and Gd@C_{82} are found to be ∼352 and 322 K, respectively. At 1 mW, κ of Dy@C_{82} is found to be 30(3) W/(m K) whereas that of Gd@C_{82} is 61(5) W/(m K). Interestingly, these values increase with increase in the laser power and thus with the local temperature, T_l. This reveals that the anharmonic coupling of vibrations in these fullerenes roots for their lattice thermal conductivity.[54]

The thermal conductivities κ of Dy@C_{82} and Gd@C_{82} are nearly 3 orders of magnitude smaller than that of graphene, graphite, and carbon nanotubes,[33,55,56] whereas they are higher than those reported for the thin films of C_{60}, C_{70}, carbon nanospheres, and amorphous carbon.[11,48,53,57,58] In pristine fullerenes, κ has mostly phonon contributions where the heat conduction occurs via lattice vibrations of covalently bonded carbon atoms.[56] However, fullerenes doped with rare-earth metals such as Dy@C_{82} and Gd@C_{82} may also have an additional

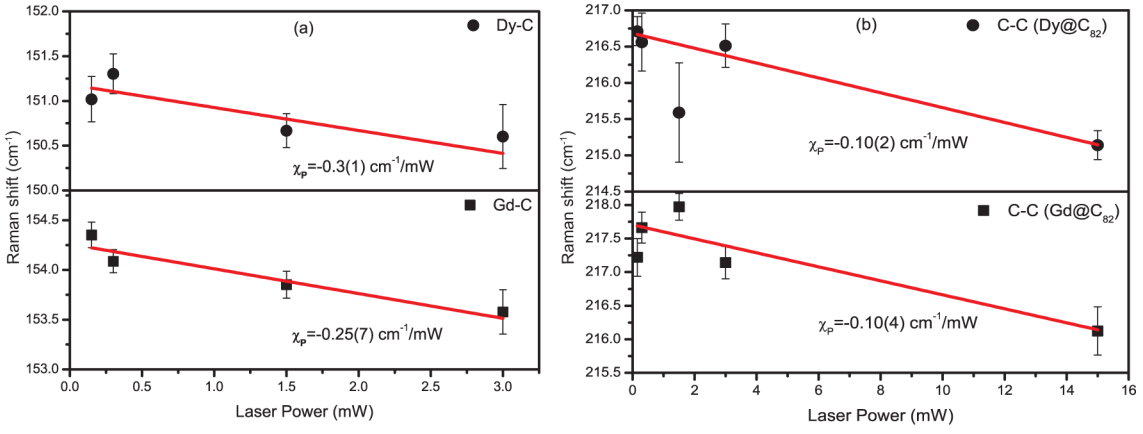

Figure 5. Laser power dependent Raman peak shift for (a) Dy−C (151 cm^{-1}) and Gd−C (154.4 cm^{-1}) modes and (b) C−C modes in Dy@C_{82} and Gd@C_{82} respectively using 785 nm excitation.

DOI: 10.1021/acs.jpcc.6b12577
J. Phys. Chem. C 2017, 121, 3642−3647

electron contribution to κ due to the presence of free charge carriers. This is why, the observed κ of Dy@C_{82} and Gd@C_{82} are higher than those of C_{60} and C_{70}. Owing to the energy transfers between C_{60}−C_{60} and C_{60}−nanotube in the carbon nanotube peapods, similar increase in the thermal conductivity is reported as compared to that of an empty tube.[12,59]

At high temperatures, phonon−phonon scattering increases which in turn limits the phonon mean free path and the thermal conductivity. In nanomaterials, both the localization of vibrations and the reduced mean free path contribute to the low thermal conductivity.[5,10,60,61] Many thermoelectric materials have shown remarkable decrease in their thermal conductivity upon being doped with C_{60} and its derivatives. Having small size and low thermal conductivity, Dy@C_{82} and Gd@C_{82} fullerenes can act as a dopant in both nano as well as bulk thermoelectric media and may offer to improve their electrical transport properties.[1,62]

CONCLUSION

In summary, temperature dependent Raman spectra of Dy@C_{82} are presented. Both metal−cage and cage internal vibrations display linear hardening with decrease in temperature and having the first order temperature coefficients χ_T −0.013(1) and −0.007 (2) cm^{-1}/K, respectively. The Raman line broadening is assigned to the contributions from both phonon−phonon and electron−phonon interactions of which the latter is dominant at low temperatures.

In addition, laser power dependent Raman spectroscopy has been employed to determine the thermal conductivity of Dy@C_{82} and Gd@C_{82} films. At 1 mW, the room temperature thermal conductivities of Dy@C_{82} and Gd@C_{82} are found to be 30(3) W/(m K) and 61(5) W/(m K), respectively. As these values increase with increase in the local temperature upon laser heating, the thermal conduction in these endohedral fullerenes is mainly attributed to the anharmonic coupling of lattice vibrations.

ASSOCIATED CONTENT

Supporting Information

The Supporting Information is available free of charge on the ACS Publications website at DOI: 10.1021/acs.jpcc.6b12577.

Dy@C_{82} and Gd@C_{82} fullerenes purification details and the plot of total angular momentum J at different temperatures for Dy@C_{82} (PDF)

AUTHOR INFORMATION

Corresponding Author

*E-mail: archana.tiwari.ox@gmail.com Phone: +91 3592 232080.

ORCID

Archana Tiwari: 0000-0002-6297-149X

Notes

The authors declare no competing financial interest.

ACKNOWLEDGMENTS

UGC-DAE-CSR Indore is thankfully acknowledged for the financial and instrumental support. AT is indebted to Dr. V Sathe, UGC-DAE-CSR, Indore for the useful discussion and help during the experiments.

REFERENCES

(1) Zhang, K.; Zhang, Y.; Wang, S. R. Enhancing Thermoelectric Properties of Organic Composites Through Hierarchical Nanostructures. *Sci. Rep.* **2013**, *3*, 3448.

(2) Medlin, D.; Snyder, G. Interfaces in Bulk Thermoelectric Materials: A Review for Current Opinion in Colloid and Interface Science. *Curr. Opin. Colloid Interface Sci.* **2009**, *14*, 226−235.

(3) Hsu, K. F.; Loo, S.; Guo, F.; Chen, W.; Dyck, J. S.; Uher, C.; Hogan, T.; Polychroniadis, E.; Kanatzidis, M. G. Cubic AgPbmSbTe$_{2+m}$: Bulk Thermoelectric Materials with High Figure of Merit. *Science* **2004**, *303*, 818−821.

(4) Zebarjadi, M.; Esfarjani, K.; Dresselhaus, M.; Ren, Z.; Chen, G. Perspectives on Thermoelectrics: From Fundamentals to Device Applications. *Energy Environ. Sci.* **2012**, *5*, 5147−5162.

(5) Kim, T. Y.; Park, C.-H.; Marzari, N. The Electronic Thermal Conductivity of Graphene. *Nano Lett.* **2016**, *16*, 2439−2443.

(6) Shi, X.; Chen, L.; Bai, S.; Huang, X.; Zhao, X.; Yao, Q.; Uher, C. Influence of Fullerene Dispersion on High Temperature Thermoelectric Properties of $Ba_yCo_4Sb_{12}$-Based Composites. *J. Appl. Phys.* **2007**, *102*, 103709.

(7) Sumino, M.; Harada, K.; Ikeda, M.; Tanaka, S.; Miyazaki, K.; Adachi, C. Thermoelectric Properties of n-type C_{60} Thin Films and Their Application in Organic Thermovoltaic Devices. *Appl. Phys. Lett.* **2011**, *99*, 093308.

(8) Popov, M.; Buga, S.; Vysikaylo, P.; Stepanov, P.; Skok, V.; Medvedev, V.; Tatyanin, E.; Denisov, V.; Kirichenko, A.; Aksenenkov, V.; et al. C_{60}-Doping of Nanostructured Bi−Sb−Te Thermoelectrics. *Phys. Status Solidi A* **2011**, *208*, 2783−2789.

(9) Popov, M.; Koga, Y.; Fujiwara, S.; Mavrin, B.; Blank, V. Carbon Nanocluster-Based Superhard Materials. *New Diamond Front. Carbon Technol.* **2002**, *12*, 229−60.

(10) Fugallo, G.; Cepellotti, A.; Paulatto, L.; Lazzeri, M.; Marzari, N.; Mauri, F. Thermal Conductivity of Graphene and Graphite: Collective Excitations and Mean Free Paths. *Nano Lett.* **2014**, *14*, 6109−6114.

(11) Tea, N.; Yu, R.; Salamon, M.; Lorents, D.; Malhotra, R.; Ruoff, R. S. Thermal Conductivity of C_{60} and C_{70} Crystals. *Appl. Phys. A: Mater. Sci. Process.* **1993**, *56*, 219−225.

(12) Vavro, J.; Llaguno, M.; Satishkumar, B.; Luzzi, D. E.; Fischer, J. E. Electrical and Thermal Properties of C_{60}-Filled Single-Wall Carbon Nanotubes. *Appl. Phys. Lett.* **2002**, *80*, 1450−1452.

(13) Shinohara, H. Endohedral Metallofullerenes. *Rep. Prog. Phys.* **2000**, *63*, 843.

(14) Popov, A. A.; Yang, S.; Dunsch, L. Endohedral Fullerenes. *Chem. Rev.* **2013**, *113*, 5989−6113.

(15) Iida, S.; Kubozono, Y.; Takabayashi, Y.; Kanbara, T.; Fukunaga, T.; Fujiki, S.; Emura, S.; Kashino, S. Structure and Electtronic Properties of Dy@C_{82} Studied by UV-VIS Absorption, X-ray Powder Diffraction and XAFS. *Chem. Phys. Lett.* **2001**, *338*, 21−28.

(16) Huang, H. J.; Yang, S. H.; Zhang, X. X. Magnetic Properties of Heavy Rare-Earth Metallofullerenes M@C_{82} (M = Gd, Tb, Dy, Ho, and Er). *J. Phys. Chem. B* **2000**, *104*, 1473−1482.

(17) Almutlaq, N.; Al-Galiby, Q.; Bailey, S.; Lambert, C. J. Identification of a Positive-Seebeck-Coefficient Exohedral Fullerene. *Nanoscale* **2016**, *8*, 13597−13602.

(18) Rincón-García, L.; Ismael, A. K.; Evangeli, C.; Grace, I.; Rubio-Bollinger, G.; Porfyrakis, K.; Agraït, N.; Lambert, C. J. Molecular Design and Control of Fullerene-Based Bi-Thermoelectric Materials. *Nat. Mater.* **2015**, *15*, 289−293.

(19) Ning, G.; Kishi, N.; Okimoto, H.; Shiraishi, M.; Sugai, T.; Shinohara, H. Structural Stability and Transformation of Aligned C60 and C70 Fullerenes in Double-Wall and Triple-Wall Carbon Nanotube-Peapods. *J. Phys. Chem. C* **2007**, *111*, 14652−14657.

(20) Kitaura, R.; Okimoto, H.; Shinohara, H.; Nakamura, T.; Osawa, H. Magnetism of the Endohedral Metallofullerenes M@ C 82 (M= Gd, Dy) and the Corresponding Nanoscale Peapods: Synchrotron Soft X-ray Magnetic Circular Dichroism and Density-Functional Theory Calculations. *Phys. Rev. B: Condens. Matter Mater. Phys.* **2007**, *76*, 172409.

DOI: 10.1021/acs.jpcc.6b12577
J. Phys. Chem. C 2017, 121, 3642−3647

(21) Rincón-García, L.; Evangeli, C.; Rubio-Bollinger, G.; Agraït, N. Thermopower Measurements in Molecular Junctions. *Chem. Soc. Rev.* **2016**, *45*, 4285−4306.
(22) Gao, Y.; Xu, B. Probing Thermal Conductivity of Fullerene C_{60} Hosting a Single Water Molecule. *J. Phys. Chem. C* **2015**, *119*, 20466−20473.
(23) Wågberg, T.; Launois, P.; Moret, R.; Huang, H.; Yang, S.; Li, I.; Tang, Z. Study by X-ray Diffraction and Raman Spectroscopy of a Dy@C_{82} Single Crystal. *Eur. Phys. J. B* **2003**, *35*, 371−375.
(24) Lebedkin, S.; Renker, B.; Heid, R.; Schober, H.; Rietschel, H. A Spectroscopic Study of M@C_{82} Metallofullerenes: Raman, Far-Infrared, and Neutron Scattering Results. *Appl. Phys. A: Mater. Sci. Process.* **1998**, *66*, 273−280.
(25) Krause, M.; Kuran, P.; Kirbach, U.; Dunsch, L. Raman and Infrared Spectra of Tm@C_{82} and Gd@C_{82}. *Carbon* **1999**, *37*, 113−115.
(26) Krause, M.; Hulman, M.; Kuzmany, H.; Dennis, T. J. S.; Inakuma, M.; H, S. Diatomic Metal Encapsulates in Fullerene Cages: A Raman and Infrared Analysis of C_{84} and Sc_2@C_{84} with D2d Symmetry. *J. Chem. Phys.* **1999**, *111*, 7976−7984.
(27) Mondal, T.; Tripathi, A.; Zhang, J.; Sathe, V.; Shripathi, T.; Shinohara, H.; Tiwari, A. Temperature-Dependent Raman Study of Gd@C_{82}. *J. Phys. Chem. C* **2015**, *119*, 12698−12702.
(28) Calizo, I.; Balandin, A. A.; Bao, W.; Miao, F.; Lau, C. N. Temperature Dependence of the Raman Spectra of Graphene and Graphene Multilayers. *Nano Lett.* **2007**, *7*, 2645−2649.
(29) Ci, L.; Zhou, Z.; Song, L.; Yan, X.; Liu, D.; Yuan, H.; Gao, Y.; Wang, J.; Liu, L.; Zhou, W. Temperature Dependence of Resonant Raman Scattering in Double-Wall Carbon Nanotubes. *Appl. Phys. Lett.* **2003**, *82*, 3098−3100.
(30) Tan, P. H.; Deng, Y.; Zhao, Q.; Cheng, W. The Intrinsic Temperature Effect of the Raman Spectra of Graphite. *Appl. Phys. Lett.* **1999**, *74*, 1818−1820.
(31) Raravikar, N. R.; Keblinski, P.; Rao, A. M.; Dresselhaus, M. S.; Schadler, L. S.; Ajayan, P. M. Temperature Dependence of Radial Breathing Mode Raman Frequency of Single-Walled Carbon Nanotubes. *Phys. Rev. B: Condens. Matter Mater. Phys.* **2002**, *66*, 235424.
(32) Perichon, S.; Lysenko, V.; Remaki, B.; Barbier, D. Measurement of Porous Silicon Thermal Conductivity by Micro-Raman Scattering. *J. Appl. Phys.* **1999**, *86*, 4700−4702.
(33) Calizo, I.; Ghosh, S.; Miao, F.; Bao, W.; Lau, c. N.; Balandin, A. A. Raman Nanometrology of Graphene: Temperature and Substrate Effects. *Solid State Commun.* **2009**, *149*, 1132−1135.
(34) Shahoo, S.; Chitturi, V. R.; Agarwal, R.; Jiang, J. W.; Katiyar, R. S. Thermal Conductivity of Freestanding Single Wall Carbon Nanotube Sheet by Raman Spectroscopy. *ACS Appl. Mater. Interfaces* **2014**, *6*, 19958−19965.
(35) Giefers, H.; Nessel, F.; Györy, S.; Strecker, M.; Wortmann, G.; Grushko, Y. S.; Alekseev, E.; Kozlov, V. Gd−L III EXAFS Study of Structural and Dynamic Properties of Gd@ C 82 Between 10 and 300 K. *Carbon* **1999**, *37*, 721−725.
(36) Jia, Y. Crystal Radii and Effective Ionic Radii of the Rare Earth Ions. *J. Solid State Chem.* **1991**, *95*, 184−187.
(37) Sobolev, B. P. *The Rare Earth Trifluorides: The High Temperature Chemistry of the Rare Earth Trifluorides*; Institut d'Estudis Catalans, 2000; Vol. *124*.
(38) Chen, L.; Chen, X.; Liu, F.; Chen, H.; Wang, H.; Zhao, E.; Jiang, Y.; Chan, T.; Wang, C.; Zhang, W. Charge Deformation and Orbital Hybridization: Intrinsic Mechanisms on Tunable Chromaticity of Y3Al5O12: Ce^{3+} Luminescence by Doping Gd^{3+} for Warm White LEDs. *Sci. Rep.* **2015**, *5*, 11514.
(39) Sahoo, S.; Gaur, A.; Ahmadi, M.; Guinel, M.; Katiyar, R. Temperature Dependent Raman Studies and Thermal Conductivity of Few Layer MoS_2. *J. Phys. Chem. C* **2013**, *117*, 9042−9047.
(40) Yan, R.; Simpson, J. R.; Bertolazzi, S.; Brivio, J.; Watson, M.; Wu, X.; Kis, A.; Luo, T.; Walker, A.; Xing, H. Thermal Conductivity of Monolayer Molybdenum Disulfide Obtained from Temperature-Dependent Raman Spectroscopy. *ACS Nano* **2014**, *8*, 986−993.
(41) Liu, M. S.; Bursill, L.; Prawer, S.; Nugent, K. W. Temperature Dependence of Raman Scattering in Single Crystal GaN Films. *Appl. Phys. Lett.* **1999**, *74*, 3125−3127.
(42) Liu, M. S.; Bursill, L.; Prawer, S. Temperature Dependence of the First-Order Raman Phonon Line of Diamond. *Phys. Rev. B: Condens. Matter Mater. Phys.* **2000**, *61*, 3391−3395.
(43) Lazzeri, M.; Piscanec, S.; Mauri, F.; Ferrari, A. C.; Robertson, J. Phonon Linewidths and Electron-Phonon Coupling in Graphite and Nanotubes. *Phys. Rev. B: Condens. Matter Mater. Phys.* **2006**, *73*, 155426.
(44) Ferrari, A. C. Raman Spectroscopy of Graphene and Graphite: Disorder, Electron-Phonon Coupling, Doping and Nonadiabatic Effects. *Solid State Commun.* **2007**, *143*, 47−57.
(45) Bonini, N.; Lazzeri, M.; Marzari, N.; Mauri, F. Phonon Anharmonicities in Graphite and Graphene. *Phys. Rev. Lett.* **2007**, *99*, 176802.
(46) Cong, C.; Yu, T. Enhanced Ultra-Low-Frequency Interlayer Shear Modes in Folded Graphene Layers. *Nat. Commun.* **2014**, *5*, 10.1038/ncomms5709
(47) Tan, P.; Han, W.; Zhao, W.; Wu, Z.; Chang, K.; Wang, H.; Wang, Y.; Bonini, N.; Marzari, N.; Pugno, N.; et al. The Shear Mode of Multilayer Graphene. *Nat. Mater.* **2012**, *11*, 294−300.
(48) Agarwal, R.; Shahoo, S.; Chitturi, V. R.; Katiyar, R. S. Graphitic Carbon Nanospheres: A Raman Spectroscopic Investigation of Thermal Conductivity and Morphological Evolution by Pulsed Laser Irradiation. *J. Appl. Phys.* **2015**, *118*, 214301.
(49) Beechem, T.; Yates, L.; Graham, S. Invited Review Article: Error and Uncertainty in Raman Thermal Conductivity Measurements. *Rev. Sci. Instrum.* **2015**, *86*, 041101.
(50) Balandin, A. A.; Ghosh, S.; Bao, W.; Calizo, I.; Teweldebrhan, D.; Miao, C. N.; Lau, F. Superior Thermal Conductivity of Single-Layer Graphene. *Nano Lett.* **2008**, *8*, 902−907.
(51) Lysenko, V.; Perichon, B.; Remaki, S.; Barbier, D. Thermal Conductivity of Thick Meso-Porous Silicon Layers by Micro-Raman Scattering. *J. Appl. Phys.* **1999**, *86*, 6841−6846.
(52) Stoib, B.; Filser, S.; Stötzel, J.; Greppmair, A.; Petermann, N.; Wiggers, H.; Schierning, G.; Stutzmann, M.; Brandt, M. Spatially Resolved Determination of Thermal Conductivity by Raman Spectroscopy. *Semicond. Sci. Technol.* **2014**, *29*, 124005.
(53) Chen, L.; Wang, X.; Kumar, S. Thermal Transport in Fullerene Derivatives Using Molecular Dynamics Simulations. *Sci. Rep.* **2015**, *5*, 12763.
(54) Foley, B. M.; Gorham, C. S.; Duda, J. C.; Cheaito, R.; Szwejkowski, C. J.; Constantin, C.; Kaehr, B.; Hopkins, P. E. Protein Thermal Conductivity Measured in the Solid State Reveals Anharmonic Interactions of Vibrations in a Fractal Structure. *J. Phys. Chem. Lett.* **2014**, *5*, 1077−1082.
(55) Hone, J.; Whitney, M.; Piskoti, C.; Zettl, A. Thermal Conductivity of Single-Walled Carbon Nanotubes. *Phys. Rev. B: Condens. Matter Mater. Phys.* **1999**, *59*, 2514.
(56) Balandin, A. A. Thermal Properties of Graphene and Nanostructured Carbon Materials. *Nat. Mater.* **2011**, *10*, 569−581.
(57) Olson, J.; Topp, K.; Pohl, R. *Phonon Scattering in Condensed Matter VII*; Springer: New York, 1993; pp 42−43.
(58) Wang, X. J.; Liman, C. D.; Treat, N. D.; Chabinyc, M. L.; Cahill, D. G. Ultralow Thermal Conductivity of Fullerene Derivatives. *Phys. Rev. B: Condens. Matter Mater. Phys.* **2013**, *88*, 075310.
(59) Noya, E. G.; Srivastava, D.; Chernozatonskii, L. A.; Menon, M. Thermal Conductivity of Carbon Nanotube Peapods. *Phys. Rev. B: Condens. Matter Mater. Phys.* **2004**, *70*, 115416.
(60) Regner, K. T.; Sellan, D. P.; Su, Z.; Amon, C. H.; McGaughey, A. J.; Malen, J. A. Broadband Phonon Mean Free Path Contributions to Thermal Conductivity Measured Using Frequency Domain Thermoreflectance. *Nat. Commun.* **2013**, *4*, 1640.
(61) Xie, G.; Guo, Y.; Wei, X.; Zhang, K.; Sun, L.; Zhong, J.; Zhang, G.; Zhang, Y.-W. Phonon Mean Free Path Spectrum and Thermal Conductivity for $Si_{1-x}Ge_x$ Nanowires. *Appl. Phys. Lett.* **2014**, *104*, 233901f.
(62) Kim, C.; Suh, D. S.; Kim, K.; Kang, Y.; Lee, T.; Khang, Y.; Cahill, D. G. Fullerene Thermal Insulation for Phase Change Memory. *Appl. Phys. Lett.* **2008**, *92*, 013109.

DOI: 10.1021/acs.jpcc.6b12577
J. Phys. Chem. C 2017, 121, 3642−3647